INVITED ARTICLE

Synthesis, characterization, and bioactivity of $SrTiO_3$-incorporated titanium coating

Souvik Sahoo
Bioceramics and Coating Division, CSIR-Central Glass & Ceramic Research Institute, Kolkata-700032, India; and Dr. M.N. Dastur School of Materials Science and Engineering, Indian Institute of Engineering Science and Technology, Howrah-711103, India

Arijit Sinha
Dr. M.N. Dastur School of Materials Science and Engineering, Indian Institute of Engineering Science and Technology, Howrah-711103, India

Vamsi Krishna Balla and Mitun Das[a)]
Bioceramics and Coating Division, CSIR-Central Glass & Ceramic Research Institute, Kolkata-700032, India

(Received 24 January 2018; accepted 2 April 2018)

Surface modification by the bioactive material is a potential way to overcome the poor osseoconductivity of titanium (Ti)-based implants. A continuous wave laser source was used to deposit strontium titanate ($SrTiO_3$)-reinforced Ti coating on the Ti substrate using the laser engineered net shaping (LENS™) process. The maximum of 10 wt% $SrTiO_3$ could be incorporated into Ti using laser without cracking of the deposit. This study investigated the constituent phases, microstructure, compositional analysis, wettability, and electrochemical behavior of the composite coatings. XRD and EDX analyses confirmed the presence of the $SrTiO_3$ phase in the coatings. The composite coatings also exhibited superior mechanical properties, corrosion resistance, and bioactivity compared to that of commercially pure Ti. In vitro ion release study confirmed the sustain release of Sr^{2+} from the composite coatings. In summary, the excellent mechanical bonding with the substrate and high in vitro bioactivity make these $SrTiO_3$-incorporated composite coatings as a potential material to enhance osseoconductivity of Ti-based orthopedic implants.

I. INTRODUCTION

Titanium (Ti) and its alloys are extensively used in orthopedic, dental, and other hard tissue replacement applications, although the low bone bonding ability of Ti is an important concern for the stability of these implants.[1] Many clinical studies showed that due to limited bioactivity of these metallic implants, dense fibrous tissue forms at the implant–bone interface,[1,2] which hinder direct bone–implant bonding. To improve the bioactivity and osseointegration, Ti implants are generally coated with bioactive materials such as calcium phosphates and bioactive glasses.[1–5] These bioactive surfaces promote formation of carbonate-substituted hydroxyapatite (HA)-like layer and ions dissolute from surface encourage osteoblast-like cells proliferation and promote osseointegration.[2,3] The clinical application of bioactive glass coatings is limited compared to HA coating, which is due to its degradation over time in physiological conditions.[2,3] Nowadays laser-based surface modification of Ti with calcium phosphate and bioactive glass coatings have been studied by several researchers.[3–7] Addition of such bioactive reinforcements can potentially improve the osteoconductivity of bioinert metallic implants. Similar observations have been reported with laser-processed calcium phosphate coatings on Ti and 316L stainless steel.[8,9] Laser deposition is also being applied to fabricate porous coatings of niobium and tantalum on Ti with high adhesion and bioactivity.[10,11] Laser-processed coatings found to have unique advantages like strong metallurgical bonding, absence of sharp interfaces, controllable concentration of reinforcements, homogeneous, fine and non-equilibrium microstructures with minimum dilution.[9,11]

Since 2004, strontium (Sr) has gained attention due to its positive role in bone remodeling. Sr is an alkaline earth metal, present nearly 0.035% of total calcium content of the mineral phase of bone.[12] Sr is also a trace element in the human body and follows almost similar metabolic pathway of calcium. Several studies showed that Sr ions stimulate the calcium sensing receptor (CaSR) in osteoblasts which activate the production of osteoprotegerin (OPG).[12] Thus the Sr ion stimulates the bone forming osteoblasts and suppresses the bone resorption and osteoclastogenesis.[12–14] Due to its dual mode of action in bone remodeling, Sr ranelate, a Sr-based drug, has been used as

[a)]Address all correspondence to this author.
e-mail: mitun@cgcri.res.in
DOI: 10.1557/jmr.2018.99

 © Materials Research Society 2018

https://doi.org/10.1557/jmr.2018.99 Published online by Cambridge University Press

an effective treatment for osteoporosis.[12] Several investigations have been carried out to utilize the stimulatory effects of Sr on bone healing and increased implant osseointegration by incorporating Sr into various biomaterials.[15–17] Sr incorporation found to promote the attachment and proliferation of osteoblast cells on calcium phosphate bone substitutes and HA coatings in vitro.[15,16] In another approach, Sr was incorporated on the surface of metallic implants to enhance the osteoconductivity of bone interfacing implants.[17–20] Forsgren et al. showed different release rates of Sr ions from a film of strontianite ($SrCO_3$) formed on sodium titanate.[18] Recent studies showed that strontium titanate ($SrTiO_3$) nanotube arrays can be fabricated on Ti using a simple hydrothermal treatment of anodized titania nanotubes.[19,20] This $SrTiO_3$ nanotube array released Sr at a slower rate for long time and demonstrated good biocompatibility.[20] Andersen et al. prepared Ti–Sr–O coatings by a magnetron co-sputtering process and demonstrated that the Sr released from the coating can significantly enhance the peri-implant bone formation after four weeks of implantation in the Wistar rat model.[21] Some studies showed that perovskite structure-like calcium titanate ($CaTiO_3$) act as the apatite growth promoter.[22] The $CaTiO_3$ phases were commonly observed in laser-deposited HA coating on Ti.[8] As per literature, no report is available till date on the use of lasers to incorporate Sr into Ti for biomedical applications. Due to its high reactivity, pure Sr cannot be incorporated in Ti. We hypothesize that the high temperature stability of Sr containing compound namely $SrTiO_3$ can be effectively incorporated into the Ti surface using direct laser deposition. In this work, Ti and $SrTiO_3$ premixed powders were melted using a high power laser to form a $SrTiO_3$-reinforced Ti matrix coatings on the Ti substrate. Such composite coatings can have reacted and unreacted Sr–Ti–O phases. In the presence of physiological solution, $SrTiO_3$-incorporated Ti coating can release Sr ions, which can potentially improve the bioactivity of Ti implants in vivo. Therefore, in the present article, we have investigated the feasibility of laser deposition of $SrTiO_3$-reinforced Ti coatings and evaluated their microstructures, electrochemical behavior, and cell–materials interactions in vitro.

II. EXPERIMENTAL

A. Composite coatings fabrication

Commercially pure Ti (CP-Ti) powder (ATI Powder Metals, Pittsburgh, Pennsylvania) of 50–150 μm size and $SrTiO_3$ powder of 2–10 μm particle sizes were used as feedstock powders. In the present work, the $SrTiO_3$ powder was prepared using strontium carbonate ($SrCO_3$, Sigma-Aldrich, Steinheim, Germany) and Ti dioxide (TiO_2, Sigma-Aldrich, Steinheim, Germany) powder. The $SrCO_3$ and TiO_2 powders in stoichiometric ratio were mixed thoroughly using ball-mill in ethyl alcohol medium and zirconium balls were used as grinding media. The milled powders were dried and fired at 1200 °C for 2 h in air. After calcinations, powders were ground and sieved to achieve $SrTiO_3$ powder with a size between 2 and 20 μm. The synthesized $SrTiO_3$ powders at varying concentrations, from 5 to 20 wt%, were thoroughly mixed with Ti powder using dilute polyvinyl alcohol solution to create premixed powders. The premixed powders were dried in a vacuum oven and sieved through 100 and 270 mesh. The premixed powders were then poured into the powder feeder of laser engineered net shaping (LENS™). A 0.5 kW continuous wave ytterbium-doped fiber laser equipped with LENS™-MR7 (Optomec Inc., Albuquerque, NM) was used to deposit 2 layers on the Ti substrate using a constant powder feed rate of 4.3 g/min. In the laser melt injection process, argon (Ar) carrier gas was used to inject the premixed powders into the molten pool created by the laser. The molten Ti and premixed powder solidify rapidly as the laser head moves on. A detailed description of the operation and capabilities of LENS™ can be found elsewhere.[23] The coatings containing 10 wt% $SrTiO_3$ found to be defect-free at optimized laser powers and scan speeds as shown in Table I. All depositions were carried out in a glove box containing an Ar atmosphere with O_2 content less than 10 ppm.

B. Microstructural, mechanical, and electrochemical behavior

Microstructural characterization of the coatings was performed using a scanning electron microscope (Phenom proX, Eindhoven, Netherlands) equipped with an energy-dispersive spectrometer. An optical microscope (BX51, Olympus, Tokyo, Japan) was used to study defects in the coatings. An X'Pert Pro MPD diffractometer with X'Celerator (PANalytical, Almelo, the Netherlands) operating at 45 kV and 40 mA with Ni-filtered Cu K_α radiation was used to determine the constituent phases in the coatings. Silicon was used as a standard for instrumental broadening correction. Vickers microhardness was measured (ESEWAY, W4303, Camberley, United Kingdom) on the top surface and cross-section of the coatings using a load of 500 g for 15 s and an average value of 15 measurements were reported. The profile of hardness across the coating thickness was determined by applying 500 g load for 10 s, and an average of ten measurements for each sample were reported. The wettability of the composite coating surfaces was determined by measuring contact angles using the sessile drop method. For contact angle measurement, the samples were mirror polished on velvet cloth using 0.05 μm Al_2O_3 suspension. An average of 10 measurements are reported for each sample.

Potentiodynamic polarization tests, conforming to ASTM G59, were performed in Hank's balanced salt

https://doi.org/10.1557/jmr.2018.99 Published online by Cambridge University Press

TABLE I. Premixed powder compositions, laser parameters, and deposited coating thickness.

Sample ID	Composition	Power (W)	Velocity (mm/s)	Energy density (J/mm^2)	Average coating thickness (μm)
Ti-10ST-200/20	Ti–10$SrTiO_3$	200	20	20	210 ± 40
Ti-10ST-250/15	Ti–10$SrTiO_3$	250	15	33.3	620 ± 50

solution, at room temperature, using a potentiostat (SP300, Bio-Logic SAS, Seyssinet-Pariset, France). A set of composite coating and CP-Ti surfaces were polished with 1 μm suspension of Al_2O_3 powder on velvet cloth and the polarisation behavior was compared with the as-deposited coating surface. All potentials were measured with respect to a saturated calomel electrode (SCE) reference electrode and platinum was used as the counter electrode for current measurement. An initial delay of 30 min prior to polarization was applied to the specimen to reach a steady-state condition at open-circuit potential (OCP). After that, the potential was increased at a rate of 10 mV/min, starting from −0.25 V to +1.6 V versus OCP. From the polarization curve, the corrosion potential (E_{corr} versus SCE) and corrosion current density (I_{corr}) were extracted by Tafel extrapolation.

C. In vitro Sr^{2+} release and cell–material interactions

The Sr^{2+} and Ti^{2+} ion release from the composite coatings were measured using inductively coupled plasma (ICP; Spectra Analytical Instrument GmbH, Kleve, Germany). The coated samples, of size 10 × 10 mm square, were ground using fine SiC grinding papers followed by ultrasonic cleaning in alcohol. After cleaning, the samples were immersed in phosphate-buffered solution (PBS) for 1, 2, 4, and 6 days at 37 °C and the extracted solutions were used for ion release study.

In vitro cytotoxicity and cell proliferation was evaluated on $SrTiO_3$-reinforced composite coatings and CP-Ti samples (control) by direct cell viability assay. Before the cell culture study, all the samples (10 × 10 mm square) were ground using 1200 series of SiC grinding papers to eliminate surface roughness effect. The polished samples were washed with water followed by alcohol and sterilized in autoclave at 121 °C for 30 min. In direct cell viability assay, human osteoblast-like cells (MG63) (NCCS, Pune, India) were seeded on polished surfaces. Cells were incubated for 2, 4, and 6 days of culture periods in a minimum essential medium, supplemented with 10% of fetal calf serum, 1% antibiotic–antimycotic solution in a humidified atmosphere at 37 °C and with 5% CO_2. The MTT [3-(4,5-dimethylthiazol-2-yl)-2,5-diphenyl tetrazolium bromide] assay was used to evaluate the cell viability. The details of MTT assay protocol can be seen elsewhere.[24]

The morphology of the cells was observed using SEM after 2 days of incubation on the test samples. The cells adhering to the samples were washed with 0.1 M PBS and fixed with 2% paraformaldehyde/2% glutaraldehyde in 0.1 M phosphate-buffered saline overnight at 4 °C. Fixed samples were then dehydrated in an ethanol series 30, 50, 70, 95, and 100% three times. Dried samples were then gold-coated and observed under an SEM. Statistical analysis was performed on the data using Student's *t*-test and $P < 0.05$ was considered statistically significant.

III. RESULTS AND DISCUSSION

A. Microstructure and phase analysis

Typical SEM micrographs of $SrTiO_3$ powder and Ti–10 wt% $SrTiO_3$ premixed powders showing their morphologies are presented in Fig. 1. The premixed powder consists of coarse spherical CP-Ti powder coated with fine $SrTiO_3$ powder. Earlier studies showed that laser deposition of premixed powders can improve homogeneous dispersion of the ceramic phase in the coating.[23,24] Figure 2 shows the cross-sectional optical microstructure of laser-processed Ti–$SrTiO_3$ composite coatings. The microstructure of the composite coatings containing 15 wt% $SrTiO_3$, shown in Fig. 2(b), exhibited cracks and gross defects. It is obvious that with increasing ceramic concentration in the metal matrix, toughness and thermal shock resistance decreases. The laser-processed coatings experience thermal shock due to fast heating and cooling rate, which generates high residual stresses. Due to deteriorating toughness of the coating containing 15 wt% $SrTiO_3$ reinforcement, unable to withstand the high residual stresses leads to cracks and gross defects. However, the composite coatings containing 10 wt% $SrTiO_3$ were relatively defect-free and showed good metallurgical bonding between the deposits and the substrate. It can be inferred from these microstructures that increasing the $SrTiO_3$ concentration from 10 to 15 wt% in the premixed powder, the coatings become brittle therefore less endurance to absorb thermal shock-related stresses, resulted in formation of cracks. Therefore, in the present investigation, Ti–10 wt% $SrTiO_3$ powder was used to fabricate composite coatings using different laser powers and scan speeds as shown in Table I. The average composite coating thickness was measured using cross sectional microstructures and the thickness was 210 ± 40 and 620 ± 50 μm for Ti-10ST-200/20 and Ti-10ST-250/15 coatings, respectively. In general, the laser-deposited layer thickness varies with laser energy input which is influenced by the laser power

https://doi.org/10.1557/jmr.2018.99 Published online by Cambridge University Press

and scan speed.[24] In the present investigation, the coating thickness increased with laser energy input and the composite coatings with 10 wt% $SrTiO_3$ prepared using 200 W and 20 mm/s (Ti-10ST-200/20) with a laser energy input of 20 J/mm^2 (Table I) showed a coating thickness of 210 ± 40 μm, which increased to 620 ± 50 μm when the laser energy input was increased to 33.3 J/mm^2 in Ti-10ST-250/15 coatings. Since all the coatings were prepared with a constant powder feed rate of 4.3 g/min, increasing the laser energy input results in bigger melt pools with higher melt temperatures on the substrate, which can accommodate and melt more amount of premixed powder that is fed to the melt pool leading to thicker coatings than observed with the coatings prepared at lower energy inputs.

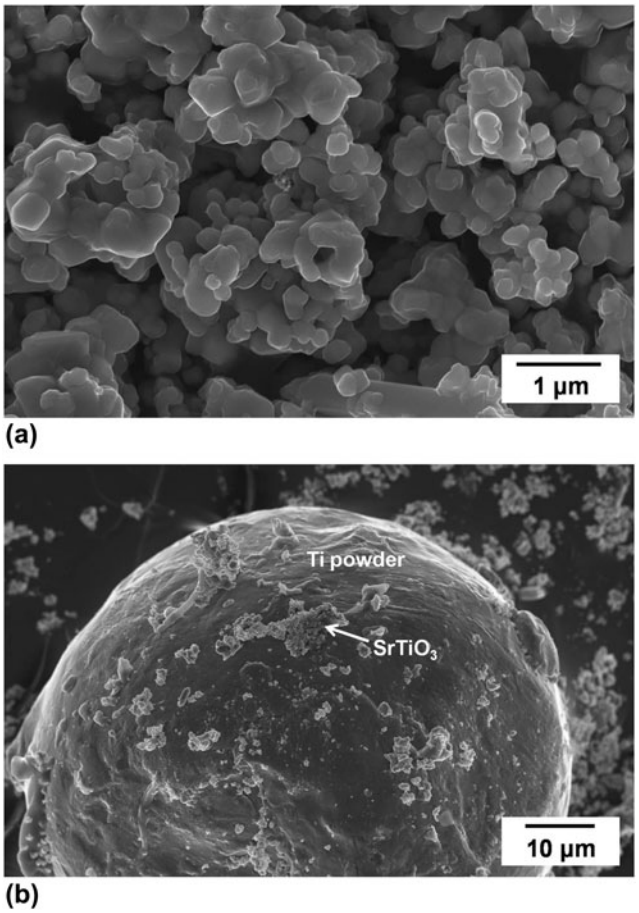


FIG. 1. SEM image of powder morphology (a) $SrTiO_3$ powders and (b) Ti–10 wt% $SrTiO_3$ premixed powders.

Figure 3 shows the top surface morphology of the 10 wt% $SrTiO_3$ reinforced composite coatings deposited using different laser powers and scan speeds. The surface roughness of these composite coatings varied between 11.6 ± 1.6 μm and 18.3 ± 1.6 μm for Ti-10ST-200/20 and Ti-10ST-250/15 coatings, respectively. The EDX analysis clearly showed the presence of Sr containing ceramic reinforcement phases on the coating's surface. The reinforcing phases, marked as spot "1" in both micrographs, were found to be depleted $SrTiO_3$ phase surrounded by the Ti matrix phase. The top surface micrograph of the Ti-10ST-250/15 coating showed high concentration of such reinforcing phases compared to Ti-10ST-200/20 coatings due to the decrease in the scan speed. The amount of powder injected into the molten pool increases with the decrease in the laser scan speed leading to high concentration of reinforcements in the composite coatings deposited at slow scan speeds.

The X-ray diffraction (XRD) patterns of synthesized $SrTiO_3$ powder, premixed powder, and laser-processed composites coatings containing 10 wt% $SrTiO_3$ are shown in Fig. 4. The XRD analysis confirmed that the synthesized powder contains pure $SrTiO_3$ phase, with no residue of reactant chemicals. The premixed powder showed both $SrTiO_3$ and Ti phases. The XRD results of polished surfaces of laser-deposited composite coatings showed predominant peaks corresponding to α-Ti and small peaks of $SrTiO_3$. The $SrTiO_3$ peaks in the Ti-10ST-250/15 coatings were more intense than those observed in the Ti-10ST-200/20 coatings and were primarily due to the increase in the concentration of the reinforcing phase in these coatings. The crystallite size of

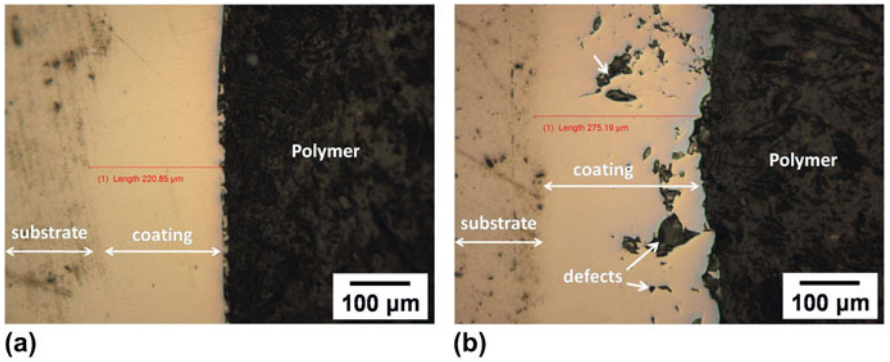


FIG. 2. Cross-sectional optical microstructures of Ti-based composite coatings with varying $SrTiO_3$, deposited at 200 W laser power and 20 mm/s scan speed (a) nearly defect-free coating, containing 10 wt% $SrTiO_3$, (b) pores and cracks in coating containing 15 wt% $SrTiO_3$.

https://doi.org/10.1557/jmr.2018.99 Published online by Cambridge University Press

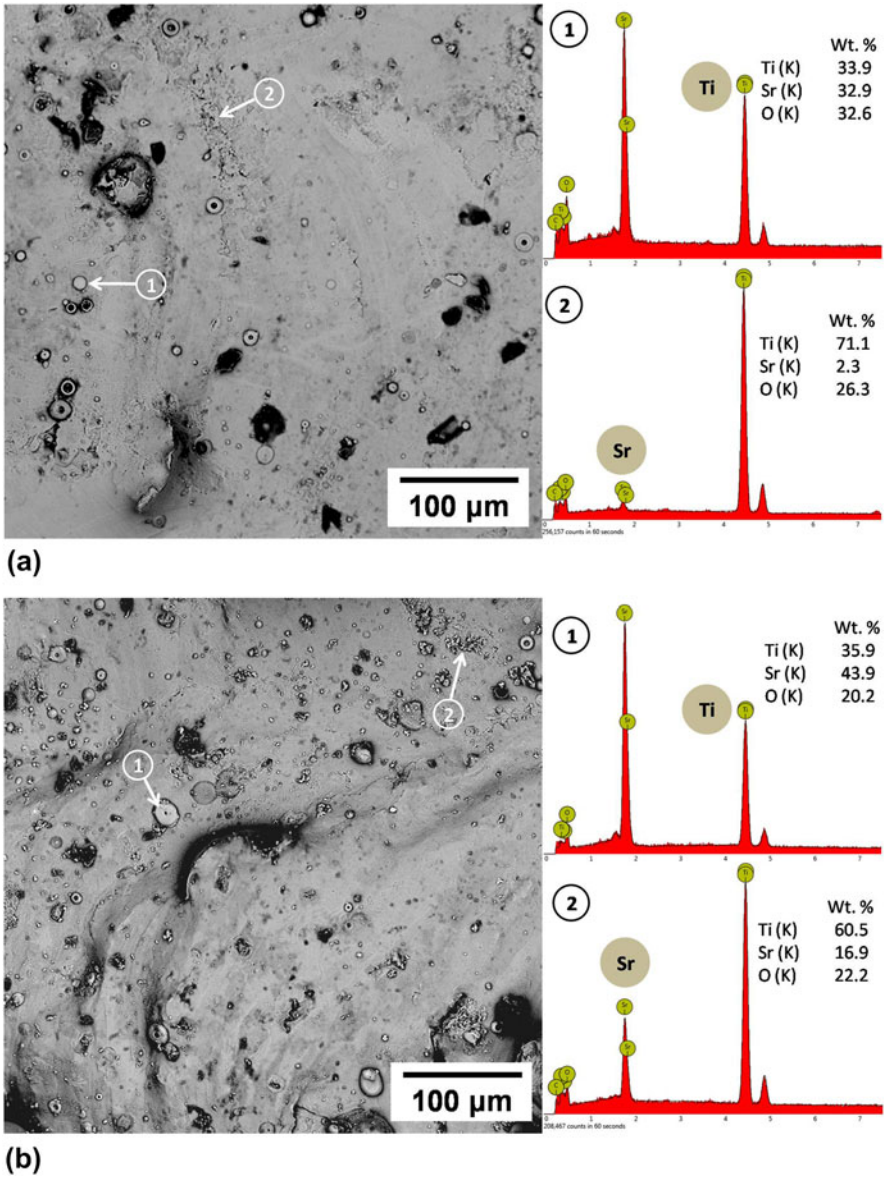


FIG. 3. Top surface microstructures of laser-processed 10 wt% $SrTiO_3$-reinforced composite coating (a) Ti-10ST-200/20 and (b) Ti-10ST-250/15.

initial $SrTiO_3$ powder and Ti crystallite size in the as-deposited coating was measured using the Scherrer equation. The crystallite size of $SrTiO_3$ powder was 340 nm and Ti crystallite size was 366 and 414 nm for Ti-10ST-200/20 and Ti-10ST-250/15 coatings, respectively.

B. Hardness, contact angle, and electrochemical behavior

Table II summaries the average top surface hardness of laser-processed $SrTiO_3$-reinforced Ti composite coatings. The experimental data indicate that the hardness of the coated surface was significantly higher than bare Ti. The high hardness in the coating is due to the presence of the hard ceramic phase in the metal matrix. Irrespective of laser parameters, the average hardness of 10 wt% $SrTiO_3$-reinforced coatings was between 491 and 507 HV. The laser parameters had no significant influence on the hardness of these composite coatings.

The wettability behavior of the biomaterial surface influences the fluid film layer and cell–material interactions. The hydrophilic nature of the surface is beneficial for cell attachment and proliferation.[11] The contact angles of water on CP-Ti and composite coatings are shown in Table II. The contact angle values measured on the coated surfaces were marginally lower than the Ti surface. The lower contact angles of composite coatings

https://doi.org/10.1557/jmr.2018.99 Published online by Cambridge University Press

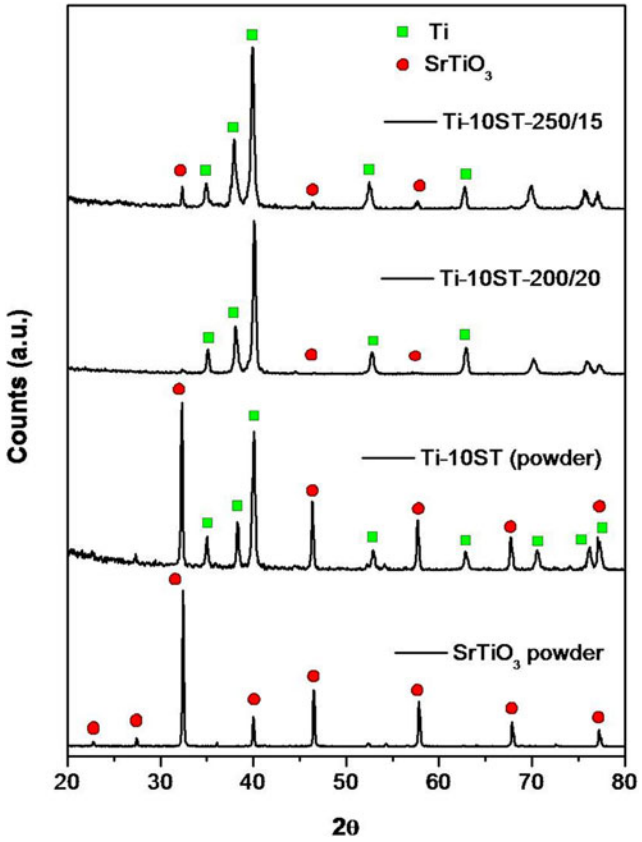


FIG. 4. XRD patterns of synthesized $SrTiO_3$ powder, Ti–$SrTiO_3$ premixed powder and laser-processed $SrTiO_3$-reinforced Ti composite coatings.

TABLE II. Average top surface hardness ($HV_{0.5}$), contact angle, and electrochemical properties of CP-Ti and $SrTiO_3$-reinforced Ti matrix composite coatings.

Sample ID	Hardness ($HV_{0.5}$), [GPa]	Contact angle (°)	Electrochemical behavior	
			E_{corr}	I_{corr} (μA)
CP-Ti	116 ± 5, [1.1 ± 0.1]	77 ± 4	−265.528	0.058
Ti-10ST-200/20	507 ± 8, [5.0 ± 0.1]	73 ± 7	−246.925	0.017
Ti-10ST-200/20 (as deposited)	...	...	−234.524	0.203
Ti-10ST-250/15	491 ± 13, [4.8 ± 0.1]	69 ± 8	−198.650	0.024
Ti-10ST-250/15 (as deposited)	...	...	−165.929	0.156

indicate their hydrophilic nature which is beneficial for cell attachment and proliferation.

The electrochemical behavior of laser-processed $SrTiO_3$-reinforced Ti matrix composite coatings was assessed using Hank's solution. Figure 5 shows the potentiodynamic polarisation curves of Ti and

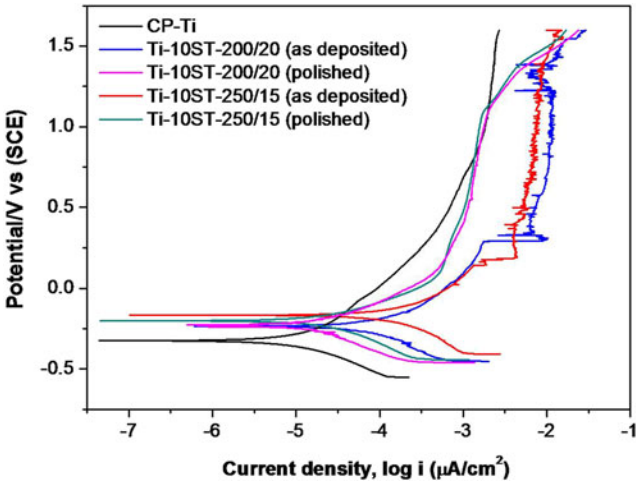


FIG. 5. Potentiodynamic polarization curves of bare Ti and 10 wt% $SrTiO_3$-reinforced composite coatings, obtained in Hank's solution.

composite coatings in polished and as-deposited conditions. The results showed higher corrosion potential (E_{corr}) for composite coatings compared to the bare CP-Ti. Higher E_{corr} of composite coatings indicates their better corrosion resistance than the CP-Ti substrate. Such an improvement in the corrosion resistance of Ti was also observed by several others when a laser-based ceramic-reinforced composite coating was applied.[25,26] The as-deposited coatings also showed higher corrosion current densities (I_{corr}) suggesting their high corrosion rates compared to respective polished surfaces. The high corrosion rate and pitting of the as-deposited coatings could be due to their rough surface leading to high surface area and leaching of Sr ions from the reinforcing ceramic phase. However, the laser parameters had no significant influence on the electrochemical behavior of these composite coatings.

C. In vitro Sr^{2+} release and cell–material interactions

Figure 6 shows the in vitro ion release from the composite coatings. The ICP analysis showed the presence of Sr^{2+} but no Ti^{2+} present in the PBS solution. The Sr^{2+} ion release was sharp up to 2 days and the release rate found less after 4 days of immersion. The Sr^{2+} ion release from Ti-10ST-250/15 composite coating was more than Ti-10ST-200/20. In case of Ti-10ST-250/15, the coating was deposited at slower scan speed leads to more amount of powder injection into the molten pool. Due to more powder, the unreacted $SrTiO_3$ phases was more in Ti-10ST-250/15 coating which was observed in SEM micrographs also. The higher amount of Sr^{2+} release in PBS solution is due to the presence of more $SrTiO_3$ in Ti-10ST-250/15 coating. The release of Sr^{2+} in vivo is desirable which

https://doi.org/10.1557/jmr.2018.99 Published online by Cambridge University Press

can significantly influence the osteoconductivity of these coatings.[21]

Cell viability and cell proliferation on $SrTiO_3$-reinforced composite coatings were carried out using human osteoblast-like cells (MG63). MTT assay was carried out to assess the cell viability on different surfaces. CP-Ti, one of the most widely used metallic biomaterial, was used as a control sample to compare the cell–material interactions. In MTT assay, optical density of the solution was measured to quantify the cell viability/living cell count. A higher optical density represents a higher concentration of living cells on the surface. Figure 7 compares the MG63 cell viability on Ti and the composite coatings surface after 2, 4, and 6 days of culture. The results indicate that the cells are viable on the composite coatings surface, irrespective of laser processing parameters. The amount of living cells on the coating surfaces was significantly higher ($P < 0.05$) than that observed on the CP-Ti only after 4 days of culture. The cell proliferation was significantly higher on the $SrTiO_3$-reinforced composite coatings compared to the control surface. The number of cells increased significantly on composite coating surfaces with culture duration. The results indicate that the presence of Sr significantly enhanced the differentiation and proliferation of osteoblast cells. Furthermore, the MG63 cell morphologies on the Ti and coating surfaces were studied after 2 days of culture, shown in Fig. 8. The cells found to grow on the Ti surface as well as on the composite surfaces and showed good adhesion and spreading. The filopodia and lamellipodia were well-established and the cells covered the entire surface. The composite coating surfaces also revealed the presence of ceramic particles which might influence the cellular activity on the coated surface. The earlier studies showed that in aqueous medium, Sr can leach from $SrTiO_3$ as partially soluble SrO and insoluble TiO_2.[19,27]

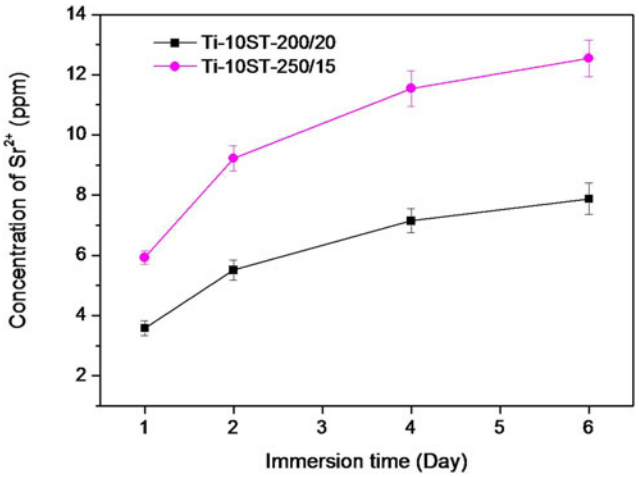


FIG. 6. Concentration of Sr^{2+} ion release from composite coatings in PBS solution at different immersion times.

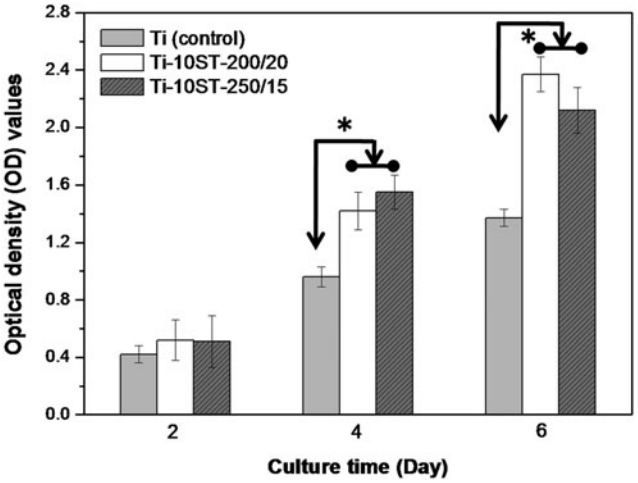


FIG. 7. MTT assay of MG63 cells observed on Ti and composite coating surfaces as a function of culture time.

$$SrTiO_3 + H_2O \rightarrow Sr^{2+} + 2OH^- + TiO_2 \quad .$$

It is clear from in vitro results that the $SrTiO_3$-reinforced composite coatings have no cytotoxicity and showed significantly high bioactivity compared to the commercial Ti. Numerous in vitro and in vivo studies have reported the stimulatory effects of Sr on osteoblastic cell responses.[21,28] Sila-Asna et al. observed that

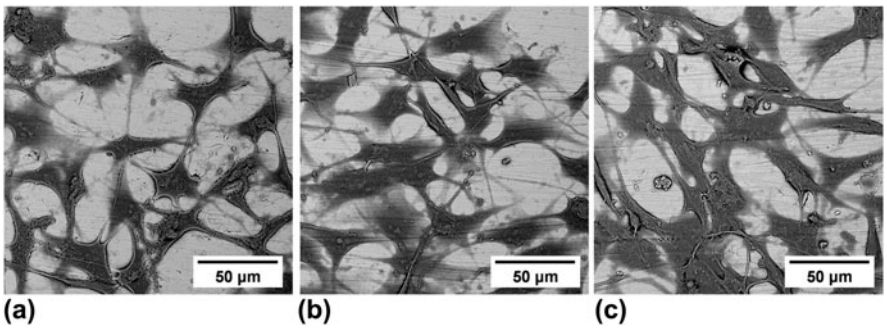


FIG. 8. SEM micrographs of MG63 cells after 2 days of culture (a) Ti control, (b) Ti-10ST200/20 coating, and (c) Ti-10ST250/15 coating.

https://doi.org/10.1557/jmr.2018.99 Published online by Cambridge University Press

osteoblastic differentiation of human bone marrow stromal cells enhanced in the presence of Sr in the cell culture medium.[29] Several researchers have suggested the probable stimulatory mechanism where Sr ion stimulates the CaSR in osteoblasts which increase the production of OPG.[12,28] Through a CaSR-mediated mechanism, Sr stimulates bone formation by increasing preosteoblastic cell proliferation and differentiation and by suppressing osteoclast differentiation. The sustain release of Sr^{2+} ions from the $SrTiO_3$-reinforced composite coating is believed to enhance the biological response of Ti-based implant for orthopedic and dental applications.

IV. CONCLUSIONS

In the current study, $SrTiO_3$-incorporated Ti matrix composite coatings were successfully deposited on the CP-Ti substrate using LENS™. The composite coating containing 10 wt% $SrTiO_3$ was defect-free and exhibited good metallurgical bonding with the substrate. EDX analysis on the top surface of the as-deposited coatings showed the presence of $SrTiO_3$ phases strongly bonded with the Ti matrix. XRD of the polished coating sample showed Ti as the main phase and small peaks of $SrTiO_3$. The average hardness of composite coatings was significantly higher than the Ti substrate. Electrochemical behavior of the composite coatings was slightly better than the Ti surface. All the coated samples showed relatively more hydrophilic compared to the Ti surface. The $SrTiO_3$-reinforced composite coatings also found to be nontoxic and showed significantly high bioactivity compared to the commercial Ti.

ACKNOWLEDGMENTS

The authors would also like to acknowledge the financial support from the Council of Scientific and Industrial Research (CSIR), India, through project ESC 0103. Mr. Souvik Sahoo is grateful to the Director, CSIR-CGCRI, Kolkata, for granting permission to carry out the entire experimental work at CSIR-CGCRI.

REFERENCES

1. J.M. Gomez-Vega, E. Saiz, and A.P. Tomsia: Glass based coatings for titanium implant alloys. *J. Biomed. Mater. Res.* **46**, 549–559 (1999).
2. F. Baino and E. Verné: Glass-based coatings on biomedical implants: A state-of-the-art review. *Biomed. Glass.* **3**, 1–17 (2017).
3. I. Cacciotti: Bivalent cationic ions doped bioactive glasses: The influence of magnesium, zinc, strontium and copper on the physical and biological properties. *J. Mater. Sci.* **52**, 8812–8831 (2017).
4. R. Comesaña, F. Quintero, F. Lusquiños, M.J. Pascual, M. Boutinguiza, A. Durán, and J. Pou: Laser cladding of bioactive glass coatings. *Acta Biomater.* **6**, 953–961 (2010).
5. S. Nag, S.R. Paital, P. Nandawana, K. Mahdak, Y.H. Ho, H.D. Vora, R. Banerjee, and N.B. Dahotre: Laser deposited biocompatible Ca–P coatings on Ti–6Al–4V: Microstructural evolution and thermal modeling. *Mater. Sci. Eng., C* **33**, 165–173 (2013).
6. G.J. Cheng, D. Pirzada, M. Cai, P. Mohanty, and A. Bandyopadhyay: Bioceramic coating of hydroxyapatite on titanium substrate with Nd-YAG laser. *Mater. Sci. Eng., C* **25**, 541–547 (2005).
7. Y. Yang, K. Serpersu, W. He, S.R. Paital, and N.B. Dahotre: Osteoblast interaction with laser cladded HA and SiO_2-HA coatings on Ti–6Al–4V. *Mater. Sci. Eng., C* **31**, 1643–1652 (2011).
8. M. Roy, V.K. Balla, A. Bandyopadhyay, and S. Bose: Laser processing of bioactive tricalcium phosphate coating on titanium for load-bearing implants. *Acta Biomater.* **4**, 324–333 (2008).
9. V.K. Balla, M. Das, S. Bose, G.D. Janaki Ram, and I. Manna: Laser surface modification of 316 L stainless steel with bioactive hydroxyapatite. *Mater. Sci. Eng., C* **33**, 4594–4598 (2013).
10. S. Zhang, X. Cheng, Y. Yao, Y. Wei, C. Han, Y. Shi, Q. Wei, and Z. Zhang: Porous niobium coatings fabricated with selective laser melting on titanium substrates: Preparation, characterization, and cell behavior. *Mater. Sci. Eng., C* **53**, 50–79 (2015).
11. V.K. Balla, S. Banerjee, S. Bose, and A. Bandyopadhyay: Direct laser processing of a tantalum coating on titanium for bone replacement structures. *Acta Biomater.* **6**, 2329–2334 (2010).
12. S. Bose, G. Fielding, S. Tarafder, and A. Bandyopadhyay: Understanding of dopant-induced osteogenesis and angiogenesis in calcium phosphate ceramics. *Trends Biotechnol.* **31**, 594–605 (2013).
13. S. Peng, X.S. Liu, S. Huang, Z. Li, H. Pan, W. Zhen, K.D.K. Luk, X.E. Guo and W.W. Lu: The cross-talk between osteoclasts and osteoblasts in response to strontium treatment: Involvement of osteoprotegerin. *Bone* **49**, 1290–1298 (2011).
14. J. Braux, F. Velard, C. Guillaume, S. Bouthors, E. Jallot, J.M. Nedelec, D. Laurent-Maquin, and P. Laquerrière: A new insight into the dissociating effect of strontium on bone resorption and formation. *Acta Biomater.* **7**, 2593–2603 (2011).
15. C. Capuccini, P. Torricelli, F. Sima, E. Boanini, C. Ristoscu, B. Bracci, G. Socol, M. Fini, I.N. Mihailescu, and A. Bigi: Strontium-substituted hydroxyapatite coatings synthesized by pulsed-laser deposition: In vitro osteoblast and osteoclast response. *Acta Biomater.* **4**, 1885–1893 (2008).
16. G.X. Ni, K.Y. Chiu, W.W. Lu, Y. Wang, Y.G. Zhang, L.B. Hao, Z.Y. Li, W.M. Lam, S.B. Lu, and K.D.K. Luk: Strontium-containing hydroxyapatite bioactive bone cement in revision hip arthroplasty. *Biomaterials* **27**, 4348–4355 (2006).
17. W. Xia, C. Lindahl, J. Lausmaa, P. Borchardt, A. Ballo, P. Thomsen, and H. Engqvist: Biomineralized strontium-substituted apatite/titanium dioxide coating on titanium surfaces. *Acta Biomater.* **6**, 1591–1600 (2010).
18. J. Forsgren and H. Engqvist: A novel method for local administration of strontium from implant surfaces. *J. Mater. Sci.: Mater. Med.* **21**, 1605–1609 (2010).
19. Y. Xin, J. Jiang, K. Huo, T. Hu, and P.K. Chu: Bioactive $SrTiO_3$ nanotube arrays: Strontium delivery platform on Ti-based osteoporotic bone implants. *ACS Nano* **3**, 3228–3234 (2009).
20. L. Zhao, H. Wang, K. Huo, X. Zhang, W. Wang, Y. Zhang, Z. Wu, and P.K. Chu: The osteogenic activity of strontium loaded titania nanotube arrays on titanium substrates. *Biomaterials* **34**, 19–29 (2013).
21. O.Z. Andersen, V. Offermanns, M. Sillassen, K.P. Almtoft, I.H. Andersen, S. Sørensen, C.S. Jeppesen, D.C.E. Kraft, J. Bøttiger, M. Rasse, F. Kloss, and M. Foss: Accelerated bone ingrowth by local delivery of strontium from surface functionalized titanium implants. *Biomaterials* **34**, 5883–5890 (2013).

https://doi.org/10.1557/jmr.2018.99 Published online by Cambridge University Press

22. J. Coreno and O. Coreno: Evaluation of calcium titanate as apatite growth promoter. *J. Biomed. Mater. Res., Part A* **75**, 478–484 (2005).
23. M. Das, V.K. Balla, T.S.S. Kumar, and I. Manna: Fabrication of biomedical implants using laser engineered net shaping (LENS™). *Trans. Indian Ceram. Soc.* **72**, 169–174 (2013).
24. M. Das, K. Bhattacharya, S.A. Dittrick, C. Mandal, V.K. Balla, T.S.S. Kumar, A. Bandyopadhyay, and I. Manna: In situ synthesized TiB–TiN reinforced Ti6Al4V alloy composite coatings: Microstructure, tribological and in vitro biocompatibility. *J. Mech. Behav. Biomed. Mater.* **29**, 259–271 (2014).
25. F. Weng, C. Chen, and H. Yu: Research status of laser cladding on titanium and its alloys: A review. *Mater. Des.* **58**, 412–425 (2014).
26. M. Das, V.K. Balla, T.S.S. Kumar, and I. Manna: Tribological, electrochemical and in vitro biocompatibility study of SiC reinforced composite coatings. *Mater. Des.* **95**, 510–517 (2016).
27. J. Anderson, B. Kahn, T. LaBone, L. Brown, and F. Harris: Solubility of various forms of strontium titanate in lungs: In vitro and in vivo studies. *Health Phys.* **76**, 628–634 (1999).
28. J.W. Park, H.K. Kim, Y.J. Kim, J.H. Jang, H. Song, and T. Hanawa: Osteoblast response and osseointegration of a Ti–6Al–4V alloy implant incorporating strontium. *Acta Biomater.* **6**, 2843–2851 (2010).
29. M. Sila-Asna, A. Bunyaratvej, S. Maeda, H. Kitaguchi, and N. Bunyaratavej: Osteoblast differentiation and bone formation gene expression in strontium-inducing bone marrow mesenchymal stem cell. *Kobe J. Med. Sci.* **53**, 25–35 (2007).

https://doi.org/10.1557/jmr.2018.99 Published online by Cambridge University Press